JOURNAL OF THE KOREAN ASTRONOMICAL SOCIETY
37: 273 ~ 279, 2004

HIGH DISPERSION OPTICAL SPECTROSCOPY OF PLANETARY NEBULAE

SIEK HYUNG
School of Science Education (Astronomy), Chungbuk National University,
12 Gaeshin-dong Heungduk-gu, CheongJu, Chungbuk 361-763, Korea
E-mail: hyung@chungbuk.ac.kr
(Received August 1, 2004; Accepted November 16, 2004)

ABSTRACT

Chemical compositions of planetary nebulae are of interest for a study of the late stage of stellar evolution and for elemental contributions to the interstellar medium of reprocessed elements since possibly a large fraction of stars in 0.8 – 8 $M_\odot$ range go through this stage. One of the methods for getting chemical composition is a construction of theoretical photoionization models, which involves geometrical complexities and a variety of physical processes. With modelling effort, one can analyze the high dispersion and find the elemental abundances for a number of planetary nebulae. The model also gives the physical parameter of planetary nebula and its central star physical parameter along with the knowledge of its evolutionary status. Two planetary nebulae, NGC 7026 and Hu 1-2, which could have evolved from about one solar mass progenitor stars, showed radically different chemical abundances: the former has high chemical abundances in most elements, while the latter has extremely low abundances. We discuss their significance in the light of the evolution of our Galaxy.

Key words : ISM: Planetary Nebula: individuals (NGC 7026, Hu 1-2, NGC 7009): Symbiotic star (AG Peg): abundances – emission spectra

I. INTRODUCTION

A star must fuse lighter elements into heavier one to maintain its life. The more mass the star has, the higher its temperature becomes and the heavier elements it fuse during the evolution. From the analysis of the spectrum of planetary nebulae (PNe), one can find the elemental abundances and get a hint of the progenitor's evolutionary history. In its main sequence life, a star fuse hydrogen to helium either p-p reaction or CN (& CNO) cycle. The latter reaction occurs only inside the star of 2 $M_\odot$ or higher, where its core temperature is higher than 1.5×10^7K. In the CNO cycle or so-called bicycle ^{16}O transform into C or N. Hence, we do not expect that N abundance enhancement from the PN which could have evolved from a star of lower than $2M_\odot$. One solar mass star like the Sun can burn helium to produce carbon, but it never reaches the high temperature enough for carbon burning. In principle, more massive massive star, viz. $>5M_\odot$, would be able to generate elements heavier than oxygen, neon and sodium and it can fuse neon. However, theoretical models of intermediate mass stars do not predict significant O or Ne production, e.g., Forestini & Charbonnel (1997). Note that sulfur is a product of oxygen burning in the life time of $>10M_\odot$ stellar evolution, while the elements near iron can only be produced from a $>20M_\odot$ star.

Planetary nebulae (PNe) are the footprints of medium stars in the mass range of 0.8 – 8 solar mass. In its main sequence life time, the progenitor star might produce the slight less heavier elements as mentioned above depending on its mass. So far, we carried out the observational program for a number of bright PNe with the Hamilton Echelle Spectrograph (HES) at Lick observatory. With modelling effort, we analyzed the high dispersion and found the elemental abundances for a number of planetary nebulae. The model also gives the physical parameter of planetary nebula and its central star along with the knowledge of its evolutionary status. Two planetary nebulae, NGC 7026 and Hu 1-2 of about the same excitation, which could have evolved from about one solar mass progenitor stars, showed a huge difference in chemical abundances and electron temperatures. We discuss the cause of this difference in the light of the evolution of our Galaxy.

The high dispersion HES data and IUE spectral data and our spectroscopic observation program are described in Section II. In Section III, the success and failure of photoionization model prediction are described. We briefly discuss the significance of the PN study in the view of the evolution of our Galaxy based on the abundances of two PNe, NGC 7026 and Hu 1-2 in Section IV.

II. SPECTROSCOPIC OBSERVATION

(a) High quality HES and IUE spectrum

Our optical spectroscopic observations were done with the HES at the Coudé focus of the 3 m Shane telescope at the Lick, whereas we used the IUE archive data for the UV spectrum. In HES observation, we employed a slit $\sim1.2''\times4''$ on the nebular image, which

Proceedings of The 2nd Korea-Mexico Joint Workshop on *Physics of the Diffuse Interstellar Medium*

corresponds to the wavelength resolution of ~0.15Å at 5000Å. The center of the slit was placed primarily at the bright blobs or at the the central star of PN (CSPN) position. Before 1995, we used the then available 800×800 CCD chip, which requires about 6 different chip settings to cover the whole optical wavelength range, i.e. 3650 – 10000Å. Although the CCD has a large dynamic range, a range of exposure times were still necessary to avoid the saturation in the strong lines and to register the weak line on a CCD. Later, we were able to to cover the whole wavelength region with the available 2048 × 2048 CCD chip. Since this large CCD chip has the same pixel size, it would have the same wavelength dispersion for the above slit entrance width. For each night, we also obtained: standard star exposures for flux calibration, e.g. 58 Aql (HR 7596) and HR 9087, a Th-Ar arc, a lamp to set wavelengths, and dome-quartz lamp exposures to fix a flat field, i.e. to allow for pixel-to-pixel sensitivity fluctuation correction. The optical wavelength spectra were reduced using the IRAF echelle reduction package, following the standard procedure of bias subtraction, aperture extraction, flat-fielding, wavelength calibration, and flux calibration. The reduction procedures are described in Hyung (1994).

The IUE spectra are available for most of our program nebulae. We used IUE spectra of low dispersion, taken through the large (10″ × 23″ oval) entrance aperture of the *IUE* cameras, which is slightly larger than or comparable to the entire nebular area in most cases. The IUE data were reduced with the NEWSIPS reduction routine at the Goddard Space Fight Center (GSFC). Hyung (1994) developed a density contrast modelling procedure to deal the different slit entrance problem used in observations even for bilaterally symmetrical objects. This modelling procedure can deal with the ionization stratification problem. Apparently, this different sampling would not be an obstacle in investigating line intensities, together. In our studies, the UV and optical line strengths were linked using the [He II] 1640/4686 ratio or the 2200Å bump to make sure two sets of data consistent. Sometimes, the former gives a higher C or A_v, then we check the continuum near the 2200Å after applying the extinction until we find the right A_v. We are ready to analyze the intensities and find the physical condition of PNe. The line intensities are further analyzed with the photoionization model to derive the abundances. We also employ a semi-empirical ICF method to avoid any serious problem introduced by the model alone.

Table 1 lists the HES optical and IUE spectrum for a symbiotic star AG Peg, PNe NGC 7026 & Hu 1-2: successive columns give the element (& ion); wavelength in Å; and the HES + IUE intensities for the objects mentioned above, respectively. The intensities are given on the scale I(4861) = 100.0, corrected for interstellar extinction assuming the extinction law of Seaton (1979). The last column lists the predicted values for Hu 1-2, which will be discussed in the next section. Column 3 of Table 1 shows that in the HES data many forbidden lines, which are seen in PNe, are missing for the case of the symbiotic star. The presence or absence of lines are closely related to the physical conditions of nebular gas, which can be investigated based on the plasma diagnostic line ratios.

(b) Plasma Diagnostics

Many lines, including those especially useful for nebular diagnostics and abundance determination, are observed in the optical spectrum of PNe (see Table 1). The HES optical spectra are mostly forbidden lines except for H I, He I and He II. They are [N II], [N III], [O II], [O III], [Ne III], [Ne IV], [S II], [S III], [Cl II],–[Cl IV], [Ar III], [Ar IV], [Ca V] and [K IV]. In the optical region, carbon lines are not present except for the permitted C II 4267. Thus, we must refer to the IUE spectra, e.g. C III] & C IV. Other IUE spectra are: He II, N III], N IV], O III, O III] and Si III].

Aller & Liller (1968, see their Fig. 1) classified the PN excitation class from 1 to 10, using the He II4686/Hβ, [O II]λ3726+3729/[O III]λ4959 and ([O III]5007+4959) /Hβ ratios. From the above ratios, NGC 7026 and Hu 1-2 can be classified as a medium excitation PN, while the mean electron temperature in the gas determined by diagnostic line ratios are very different. Line ratios which fix T_ϵ are [N II](6548+6584)/5755, [Ar III] (7751+7136)/5192, [O III](4959+5007)/4363, [S III] 9069/6312, [Ar IV](4740+4711)/7171, [Cl IV] 8046/5324, etc. The temperature sensitive diagnostic lines indicate that NGC 7026 has relatively low electron temperatures of around T_ϵ = 8000 – 9500 K, while Hu 1-2 has very high T_ϵ = 12 000 – 18 000 K. Line ratios suitable for fixing N_ϵ are [N I]5198/5200, [S II]6731/6716, [O II] 3726/3729, [Cl III] 5538/5518, [Ar IV] 4740/4711, etc. These diagnostics indicate that both PNe have electron densities of $N_\epsilon \sim$ 3000–10 000 cm^{-3}. At first sight, it is hard to understand this large temperature difference for the similar excitation class PNe.

With the forbidden lines involving p^3 electrons, one can also obtain diagnostics for both density and temperature at the same time (see Keenan et al. 2003; 2000) (1) [O II]: λ3729/λ3726 vs. λ7320,7330/(λ3726 + λ3729); (2) [Ar IV] λ4711/λ4740 vs. λ7171/(λ4711 + λ4740); [Ar IV] λ4711/λ4740 vs. λ7263/(λ4711 + λ4740); (3) [S II]: λ6716/λ6731 vs. λ4068,4076/(λ6716 + λ6731). As pointed out in Hyung, Aller & Feibelman (2001), the electron temperatures indicated by these p^3 diagnostics may incur a relatively large error, due to the crowding of temperature diagnostic lines, whereas the density diagnostics seem to be useful.

Once we find the physical condition, the ionic concentrations can be obtained by well-known formulae, see e.g. Aller (1984), updated with the most recent and reliable values of the atomic constants. A compilation of recent electronic collision strengths is given in our earlier studies, e.g. Hyung and Aller (1996). In de-

TABLE 1
LINE INTENSITIES AND PHOTOIONIZATION MODEL PREDICTION

El–ion	λ(Å)	I(AG Peg)	I(7026)[a]	I(Hu1-2)[b]	Model[c]
He I	5876	22.6-19.1	11.51	10.06	9.33
	6678	23.8-19.5	–	2.44	2.09
	4471	3.05-4.05	3.85	2.68	3.35
He II	4686	115-31.2	88.76	73.84	83.71
	5412	6.30-3.73	5.44	5.95	7.20
	1640	[774]		[604]	632
C II	2325/28	–		[83.8]	54.7
	4267	0.58-0.09	–	0.09	
C III	1907/09	[193.9]		[441]	560
C IV	1548/51	[627]		[712]	505
N II	6584	–	241.7	171.1	158.6
	6548	–	71.76	58.96	54.75
	5755	–	5.67	5.67	6.02
N III	1747-52	[181]		[171]	134
N IV	1483/86	[388]		[256]	91.7
N V	1239/42	–		[243]	28
O I	6300	0.55-0.56	–	6.67	0.14
	6363	–	2.81	2.12	0.05
O II	3726	1.37-3.15	–	31.94	29.31
	3729	0.87-1.41	14.94	14.42	12.68
	7321/2	–	4.24	4.55	3.91
	7332/3	–	3.18	3.97	3.13
O III	1660/66	[372]		[45]	39
	4363	2.26-0.71	24.57	25.65	14.86
	4959	–	279.0	221.4	254.1
	5007	–	823.3	717.0	731.9
Ne III	3868	1.07-0.54	86.90	70.27	81.62
	3968	0.93-0.11	27.57	26.37	24.36
Ne IV	4725/27	1.37-0.04	2.23	2.96	0.53
S II	4068	0.63-0.11	3.41	3.30	1.48
	4076	0.61-0.006	0.99	1.19	0.50
	6717	–	6.17	5.42	1.30
	6731	–	11.92	11.02	2.39
S III	6312	–	2.14	3.48	1.88
	9069	–	14.86	13.38	18.96
	9531	–	36.97	21.54	46.20
Cl II	8579	–	–	0.16	0.17
Cl III	5518	–	0.50	0.48	0.49
	5538	–	0.71	0.59	0.78
Cl IV	7530	–	0.48	0.46	0.35
	8046	–	0.84	0.87	0.87
Ar III	5192	–	0.25	0.29	0.20
	7136	–	11.81	10.96	12.86
	7751	–	–	2.18	3.11
Ar IV	4711	1.24-0.044	5.65	4.25	4.40
	4740	–	5.45	6.51	5.92
	7238	–	0.37	0.37	0.16
	7263	–	–	0.31	0.18
	7171	–	–	0.28	0.22
Ca V	5310	–		0.13	0.17
K IV	6102	–		0.30	0.35
Si III	1883/92	[141]		[37]	36.5

The optical wavelength spectra are those of HES, while the UV spectra are from the IUE Archive data, whose line strengths are linked with the HES using the theoretical He II 1640/4686 ratios (listed in square brackets). I(AG Peg): HES data in 1998, 2001 & 2002 ($A_v = 0.08$). [a]: from HF. [b]: from HPF. [c]: Model for Hu 1-2 (HPF).

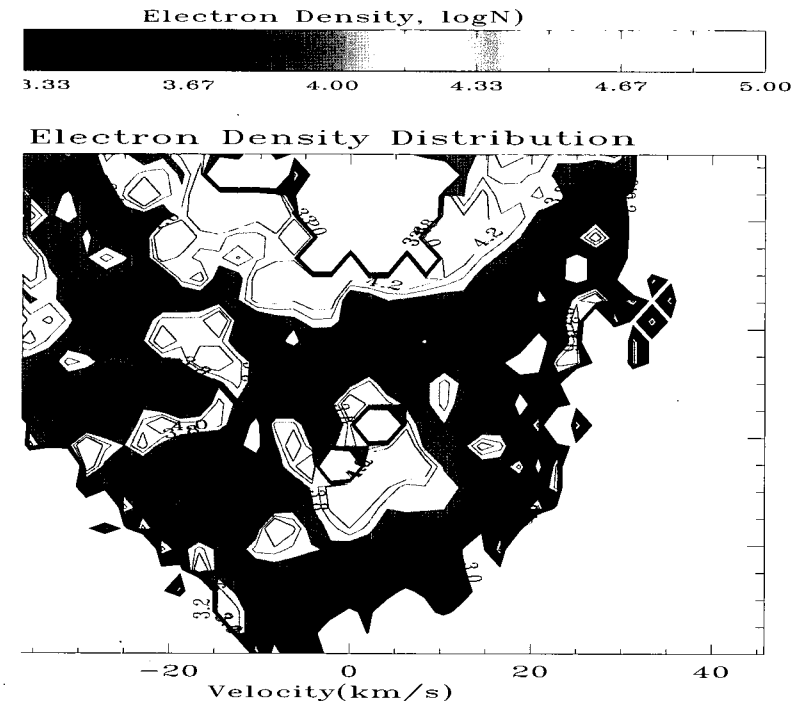

Fig. 1.— Density structure: spatial vs. velocity component (NGC 7009). The direction of slit length on a nebular image corresponds to the vertical axis.

riving ionic concentrations, we rely on the value derived based on the optical lines, but sometimes we refer to the IUE measurements, whenever they are available. To determine the abundance of PNe, we must use the Ionization Correction Factors (ICF's) for the unobserved ionic stages. Models give the ionic concentrations for all of the ionization stages including unobserved ionic stages, so one can find the ICF by checking the model predicted fraction of the unobserved ionic stages relative to that of the observed ones.

It is questionable whether the electron temperatures and densities determined in the above represent the whole PN, especially when the stratification effects are serious. We then expect that there will be a large positional variation of physical condition and different line intensities are expected. We must consider that there is an observation bias in the spectra, depending on the selected position over the nebular image: relatively high excitation lines such as [O III] and [Cl IV], will be stronger at the central position, whereas low excitation lines such as [O II] and [Cl III] will be relatively weaker, there. Hence, we need to construct a theoretical model which accommodates such a complicated situation.

III. PHOTOIONIZATION MODEL

To understand the physical condition of the PNe in a more self-consistent way, we construct a photoionization (P-I) model. The P-I code employed in our study was developed by Hyung (1994) to study the line intensities even for bilaterally symmetric compact objects with a large density contrast, see e.g. Hyung and Aller (1996). To a first approximation, the correct value of the distance to the PN is not critical in fitting the line intensities. However, one must narrow it down to a reasonable range, since only the correct distance would give an appropriate physical scale for both the CSPN and the PN. We adopted distances of ~2.0 kpc for NGC 7026, close to the derivation of 2180 (±700) pc by Solf & Weinberger (1984), and 1.5 kpc for Hu 1-2 (see Hajian & Terzian 1996).

The CSPN temperature must be determined along with the nebular geometry. In our construction, we directly employ various central star temperatures until we find the right temperature which predicts the observed physical condition of the PN. Hubeny's (1980) theoretical model atmosphere code was used to generate the CSPN spectral energy distribution (SED), for each T_{eff} and log g. This method is similar to the energy-balance and Zanstra methods for the CSPN temperature derivation. Once we find the approximate value for the CSPN, we further refine the nebular model calculation until it fits the other observed quantities. From such an effort, we determine the CSPN temperature of NGC 7026 and Hu 1-2 as $T_{eff} \sim 80\,000$ K & 125 000 K, respectively (see Hyung & Feibelman 2004;

TABLE 2
ABUNDANCES FOR NGC 7026 AND HU 1-2

Elem	NGC 7026[a]	Hu 1-2[b]	Mean[c]	Sun[d]
He	0.115	0.13	0.11	0.086
C	9.00(-4)	1.6(-4)	6.48(-4)	2.57(-4)
N	4.75(-4)	1.8(-4)	1.40(-4)	6.31(-5)
O	7.00(-4)	1.3(-4)	4.93(-4)	4.57(-4)
Ne	1.70(-4)	4.9(-4)	1.25(-4)	6.92(-5)
S	1.90(-5)	3.5(-5)	8.08(-6)	2.14(-5)
Ar	5.20(-6)	1.1(-6)	2.42(-6)	1.51(-6)
Cl	3.60(-7)	1.1(-7)	1.66(-7)	3.16(-7)
K	5.00(-8)	9.0(-8)	...	1.35(-7)
Si	1.80(-5)	0.5(-5)	...	3.55(-5)

X(-Y) means X $\times$ 10^{-Y}. All abundances are given relative to $N(H^+)$. [a] Hyung & Feibelman (2004, HF). [b] Hyung, Pottasch & Feibelman (2004, HPF). [c] Average (or normal) abundances from Kingburgh & Barlow (1994) [d] Solar abundances are from Christensen-Dalsgaard (1998) for He; Asplund (2003) for C & N; Asplund et al. (2004) for O, Ne & Ar; and Grevesse & Sauval (1998) for others, respectively.

Hyung, Pottasch & Feibelman 2004).

For the CSPN SED calculation, we also used the same He/H and heavy element distribution in the central star as in the nebular gas. Since the model geometry is spherical, one expect an error in the abundance derivation. Nonetheless, the modelling procedure which represents the complicated real situation and line diagnostic information, appears to be the best way of getting the abundance determination. The nebula is assumed to be a homogeneous shell with the gas density adopted from the diagnostic information. As an example, we give the predictions for Hu 1-2 in the last column of Table 1. Although the model generally reproduces most of lines and the nebular physical conditions derived from the spectral data analysis, the employed spherical model cannot accommodate the bipolar or non-spherical appearances. The photoionization model can globally predict the electron temperatures indicated by [N II], [Ar III] and [O III], although it cannot predict the large scatter suggested by other faint ions.

The prediction for the [S II] lines, which might have formed in or near the neutral cloud region, has a problem (see Table 1). One cannot attribute this [S II] problem to the improper model. If then, most of the other lines must disagree. The atomic constant would not be a problem (see Keenan et al. 1996), either. In our previous observation for other objects, we also note the enhancement of [S II] and [O I]. In fact, the predicted [S II] values seem to be always weaker. We suspect that a large fraction of emission has been formed through shock excitation. To verify this, we used the long slit and high dispersion capability of Keck HIRES. The Keck HIRES relatively longslit was placed along the minor axis of NGC 7009 image and carried out observation in 1998. Figure 1 shows the derived density vs. velocity dispersion 2D plot. Here, the density was derived from the [S II]6716/6731 ratio, while the velocity dispersion, $\triangle V \simeq 20 - 40$ km s^{-1}, was obtained from the 2-D (wavelength, spatial) dispersion of the emission lines: the top of box in Figure 1 corresponds to center of the NGC 7009 image, showing the front and rear shells are approaching and receding, respectively; the low part of the box is the kinematics for the bright rim, expanding tangential to the observer. Meanwhile, the other low excitation [O II] 2-D diagram indicates that the shell of this emission region simply expands at 20 km s^{-1} and does not show the similarly large velocity scatter.

The prediction for the permitted C II λ4267 is also a headache. It has been a well-known problem for a long time that the photoionization model with the same abundance adopted for the forbidden line, cannot predict both the permitted and forbidden lines at the same time. If one tries to predict the C II λ4267, as a recombination mechanism, the prediction will be 3–10 times weaker. Thus, we also need to consider other emission mechanisms responsible for this and other permitted lines. For example, it might be produced by a fluorescence or a scattering mechanism. The other possibility is the so-called temperature fluctuation (Peimbert et al. 1995) or density fluctuation. Since the employed photoionization model is a simplified homogeneous shell, it does not admit a point-to-point fluctuation of N_ϵ and T_ϵ. In Table 1, the symbiotic star AG Peg shows a number of forbidden lines, but many more numerous permitted lines are observed. It would be worth while to study the permitted lines of symbiotics with the photoionization model, and compare them with the PN case.

Based on the model, we are then able to derive the abundances for PNe. We summarize the abundances of NGC 7026 and Hu 1-2 in Table 2. For each element in column 1, the derived abundances (in columns 2 & 3) can be compared with the average value for PNs (in column 4) and the Sun (column 5) to enlighten their meaning in the evolutionary history of the Galaxy. For NGC 7026, the C, N, O, Ne, S, and Ar abundances are highly enhanced, whereas other rare elements, K, Si, and probably Cl appear to be depleted. These highly enhanced chemical abundances are the main cause of the relatively low gas temperatures. Meanwhile, Hu 1-2 has the lowest abundance ever found by us, except for He and N. The abundances are even lower than the solar values. Carbon, oxygen, neon, sulfur and argon are not produced in the PN progenitor in the course of its low mass star evolution, and instead they reflect the previous generation which perished now, i.e. abundances in the current PN's progenitor's star formation history.

IV. DISCUSSION

For the adopted distance, we further refine the model, scaling the CSPN properties and nebular size to reproduce the absolute Hβ flux to within observational errors. We are then able to find a central star radius and its luminosity. We found $R_* = 0.24R_\odot$ & $L_* = 2400\ L_\odot$ for NGC 7026; and $R_* = 0.056R_\odot$ & $L_* = 700\ L_\odot$. Taking L($\star$) and T($\star$) at their face values, and utilizing Schönberner's (1989) evolutionary tracks, we can derive a CSPN mass, viz. 0.56 $M_\odot$ for both NGC 7026 & Hu 1-2. The progenitors must have been slightly less massive than our Sun on their main sequence phase, which indicates that both objects are more than 10 billion years old.

Note that the low mass star cannot produce heavy elements during its evolutionary life. However, the chemical abundances of NGC 7026 are highly enhanced than the average PN or the Sun. This gives troubles for the evolutionary scenario based on a simple single star evolution. We know the PNe are the 3rd generation, while the Sun is the 4th generation probably borne after $\sim$5 billion years after two PNe. The possible explanation is that the progenitor of NGC 7026 was borne from the already chemically enriched gas by a previous generation of stars, perhaps near or in the Galactic plane.

The distance adopted for NGC 7026 is basically a statistical distance, whereas that for Hu 1-2 is based upon an expansion parallax. The latter is likely to be reliable, the former likely to be highly unreliable. Note the other evidence available for both objects. Hu 1-2 is elliptical, observed 10 degrees above the galactic plane, of small angular size (6″), and has a radial velocity very different from that of the ISM in its direction. The angular size and adopted distance imply a physical size of 0.04 pc. All of these characteristics are reasonable for a planetary nebula derived from a low mass, metal-poor progenitor, and in agreement with the low abundances observed. In contrast, NGC 7026 is highly resolved, reasonably large (43"), almost exactly in the galactic plane, and has an observed radial velocity in good agreement with that of the ISM along its line of sight. The angular size and adopted distance imply a physical size of 0.42 pc. These properties are inconsistent with a planetary nebula derived from a low mass progenitor whose central star is furthermore supposed to be still on the horizontal part of its post-AGB evolution in the HR diagram. Far more likely is that the distance is wrong. If NGC 7026 is much nearer, its central star would then require a temperature and luminosity that would likely place it on the descending part of the post-AGB evolutionary track, in agreement with its highly structured nebula that would then also have a more typical $\sim$0.1 pc size. Were this the case, and NGC 7026 derived from a more massive progenitor, its bipolar or multi-polar morphology, its abundances exceeding the solar values, its position and kinematics in the galactic plane, are all easily understood.

The other possibility is that the CSPN of NGC 7026 is evolved from a massive progenitor in a binary system, of which a large mass fraction was already transferred into the other (unobservable) companion. It would be worth while to investigate this binary possibility and the bipolar morphology. In this study, we did not construct a model for the symbiotic star AG Peg. If NGC 7026 is evolved from a binary system like the symbiotic star AG Peg, the model study of symbiotic star might enlighten or clarify many PN issues and problems, e.g. Peimbert type I PN (Peimbert et al. 1995), dredge-up process and shaping scenario. On the other hand, the Hu 1-2 progenitor or its YSO might have been formed in a chemically uncontaminated region of the Galaxy, e.g. near the Galactic halo. We must postpone our conclusion till more appropriate distance is found.

ACKNOWLEDGEMENTS

This work was supported by Chungbuk National University Grant in 2004. We thank Dr. Michael Richer (IA-UNAM, Ensenada) for his careful review and valuable comments.

REFERENCES

Aller, L. H. 1984, Physics of Thermal Gaseous Nebulae, (Dordrecht: Reidel Publishing Company)

Aller, L. H., & Liller W. 1968, in Middlehurst B.M. and Aller, L.H., eds, Nebulae and Interstellar Matter, University of Chicago Press, Chicago, ch. 9, p498

Asplund, M. 2003, in CNO in the Universe, eds. C. Charbonnel, D. Schaerer, & G. Meynet, ASP Conference Series, 304, 275

Asplund, M., Grevesse, N., Sauval, A. J., Allende Prieto, C., & Kiselman, D. 2004, A&A, 417, 751

Christensen-Dalsgaard, J. 1998, Space Sci., 85, 19

'Forestini, M., & Charbonnel, C. 1997, A&AS, 123, 241

Hajian, A.R., & Terzian, Y. 1996, PASP, 108, 258

Hubeny, I. 1988, Computer Phys. Comm., 52, 103

Hyung, S. 1994, ApJS, 90, 119

Hyung, S., & Aller, L. H., 1996, MNRAS, 278, 551

Hyung, S., Aller, L. H., Feibelman, W. A., & Lee, S.-J. 2001, ApJ, 563, 889

Hyung, S., & Feibelman, W. A. 2004, ApJ, 614, 745

Hyung, S., S. R. Pottasch, & Feibelman, 2004, A&A 425, 143

Keenan, F. P., Aller, L. H., Exter, K. M., Hyung, S., & Pollacco, D. L. 2003, ApJ, 584, 385

Keenan, F. P., Aller, L. H., Bell, K. L., Hyung, S., McKenna, F. C. Ramsbottom, C. A. 1996, MNRAS, 281, 1073

Keenan, F. P., Aller, L. H., Ramsbottom, C. A., Bell, K. L., Crawford, F. L., & Hyung, S. 2000, Proc. Natl. Acad Sci. USA, 97, 4551

Peimbert, M., Luridiana, V., & Torres-Peimbert, S. 1995, RMxA&A, 31, 147

Robberto, M., Stanghellini, M., Ligori, S., Herbst, T. M., & Thompson, D. 1997, in IAU Symposium 180, Planetary Nebulae, ed. D.R. Flower (Dordrecht: Reidel), p. 275

Schönberner, B. 1989, in IAU Symp. 131, Planetary Nebula. ASP Conference series, Ed. S. Torres-Peimbert (Dordrecht) p. 463

Seaton, M. J. 1979, MNRAS, 187, 73p

Solf, J., & Weinberger, R. 1984, A&A, 130, 269